ON THE EFFECT OF DAMPING AND CONTROLS ON AN AIRCRAFT WAKE ENCOUNTER

L.M.B.C. Campos, J.M.G. Marques
Secção de Mecânica Aeroespacial, Instituto Superior Técnico, 1049-001 Lisboa, Portugal

Keywords: *Wake Encounter, Safety Distances, Aircraft Response*

Abstract

The effect of damping and controls on an aircraft wake encounter is modeled using the following assumptions: (i) the wake of the leading aircraft is represented by a pair of counterotating Hallock-Burham vortices, with arbitrary circulations and core radii; (ii) the vorticity decays with distance due to a turbulent kinematic viscosity, according to a law which is consistent with flight data from the Memphis data base; (iii) the rolling moment induced in the following aircraft is calculated assuming it flies aligned behind the leading aircraft; (iv) the rolling moment equation is solved analytically including the effect of the control surface deflection (e.g. ailerons) and of aerodynamic damping; (v) the airplane response, in terms of roll rate and bank angle is plotted for a Boeing B757-200 flying behind another. It is shown that in the absence of control action, the roll rate of the following aircraft goes through a peak, and then decays, leading to a constant asymptotic bank angle; the latter is a measure of the magnitude of the wake effect, e.g. is larger for weaker damping. The exact analytical solution of the roll equation appears as a power series of a damping factor, whose coefficients are exponential integrals of time; it is shown that the first two terms give an accuracy better than 2%.

1 Introduction

The effect of damping and controls on an aircraft wake encounter is modeled using the following assumptions: (i) the wake of the leading aircraft is represented by a pair of counterotating Hallock-Burham vortices, with arbitrary circulations and core radii; (ii) the vorticity decays with distance due to a turbulent kinematic viscosity, according to a law which is consistent with flight data from the Memphis data base; (iii) the rolling moment induced in the following aircraft is calculated assuming it flies aligned behind the leading aircraft; (iv) the rolling moment equation is solved analytically including the effect of the control surface deflection (e.g. ailerons) and of aerodynamic damping; (v) the airplane response, in terms of roll rate and bank angle is plotted for a Boeing B757-200 flying behind another. It is shown that in the absence of control action, the roll rate of the following aircraft goes through a peak, and then decays, leading to a constant asymptotic bank angle; the latter is a measure of the magnitude of the wake effect, e.g. is larger for weaker damping. The exact analytical solution of the roll equation appears as a power series of a damping factor, whose coefficients are exponential integrals of time; it is shown that the first two terms give an accuracy better than 2%.

2 Rolling Moment Induced by vortex pair

The main effect of the wake of a leading aircraft on a following is to induce [7] a rolling moment:

$$R = -\frac{1}{2} C_{L_\alpha} \rho U \int_{-b/2}^{b/2} y\, c(y) w(y)\, dy, \quad (1)$$

the chord is a linear function of spanwise coordinate [8] for a trapezoidal wing

$$c(y) = \frac{2\bar{c}}{1+\lambda}\left[1 + \frac{(\lambda-1)}{b} 2|y|\right], \quad (2)$$

where the mean geometric chord $\bar{c}$ and taper ratio λ are specified by the root c_r and tip c_t chords:

$$2\bar{c} \equiv c_t + c_r, \qquad \lambda \equiv \frac{c_t}{c_r}. \tag{3a,b}$$

It remains to specify the downwash $w(y)$, which depends on the vortex model assumed.

For an Hallock-Burnham (HB) vortex [20] the tangential velocity is given by:

$$w_0(r) = \frac{\Gamma_0}{2\pi}\frac{r}{r^2+a^2}, \tag{4}$$

where the vorticity may be introduced for the peak velocity at the vortex core radius:

$$\Omega a/4 = w_{0\max} \equiv w_0(a) = \Gamma_0/4\pi a. \tag{5}$$

Instead of a single HB-vortex:

$$2w_0(r) = \frac{\Omega a^2 r}{r^2+a^2}, \tag{6}$$

the wake of the leading aircraft is represented (*Figure 1*) by a pair of possibly dissimilar HB-vortices, with vorticities $\Omega_r, -\Omega_l$, core radii a_r, a_l and axis at y_r, y_l parallel to the flight path:

$$2w(y) = \Omega_r a_r^2 \frac{y-y_r}{a_r^2+(y-y_r)^2} - \Omega_\ell a_\ell^2 \frac{y-y_\ell}{a_\ell^2+(y-y_\ell)^2}, \tag{7}$$

and lying at the same altitude. The correction to (7) has been given [21] when the aircraft is not at the same altitude as the vortex core centers or has a bank angle. Substitution of (2) and (7) in (1) specifies the rolling moment for any spanwise vortex pair position, i.e. either vortex within, outside or partly inside the span of the following aircraft.

The rolling moment (1) is specified by:

$$2R = -\frac{C_{L_\alpha}\rho U\bar{c}\Omega_r a_r^2}{1+\lambda}\int_{-b/2}^{b/2} y\left(1+\frac{\lambda-1}{b}2|y|\right)\frac{y-y_r}{a_r^2+(y-y_r)^2}dy + \frac{C_{L_\alpha}\rho U\bar{c}\Omega_l a_l^2}{1+\lambda}\int_{-b/2}^{b/2} y\left(1+\frac{\lambda-1}{b}2|y|\right)\frac{y-y_l}{a_l^2+(y-y_l)^2}dy. \tag{8}$$

The rolling moment is thus given by:

$$R = -\frac{C_{L_\alpha}\rho U\bar{c}b}{1+\lambda}\left(\Omega_r a_r^2 h_r - \Omega_l a_l^2 h_l\right), \tag{9}$$

where h_r is a dimensionless factor:

$$4h_r = J_{1r} + (\lambda-1)J_{2r}, \tag{10}$$

involving the integrals:

$$J_{1r} \equiv \frac{2}{b}\int_{-b/2}^{b/2}\frac{y(y-y_r)}{a_r^2+(y-y_r)^2}dy, \tag{11a}$$

$$J_{2r} \equiv \frac{4}{b^2}\int_{0,0}^{b/2,-b/2}\frac{y^2(y-y_r)}{a_r^2+(y-y_r)^2}dy, \tag{11b}$$

where the second integral is evaluated twice at each limit. Corresponding formulas apply to h_l, and a similar change of variable, allows elementary evaluation of the integrals:

$$u \equiv (y-y_r)/a_r: \quad J_{1r} = \frac{2}{b}\int_{-(b/2+y_r)/a_r}^{(b/2-y_r)/a_r}\frac{u(y_r+a_r u)}{1+u^2}du = \left[\frac{y_r}{b}\log\left(1+u^2\right)+2\frac{a_r}{b}(u-\arctan u)\right]_{-(b/2+y_r)/a_r}^{(b/2-y_r)/a_r},$$

$$J_{2r} = \frac{4}{b^2}\int_{-y_r/a_r,-y_r/a_r}^{(b/2-y_r)/a_r,-(b/2+y_r)/a_r}\frac{y_r^2 u + 2y_r a_r u^2 + a_r^2 u^3}{1+u^2}du = 2\left[\left(\frac{y_r^2-a_r^2}{b^2}\right)\log\left(1+u^2\right) + 4\frac{a_r y_r}{b^2}(u-\arctan u) + \frac{a_r^2}{b^2}u^2\right]_{-y_r/a_r,-y_r/a_r}^{(b/2-y_r)/a_r,-(b/2+y_r)/a_r}.$$

Substitution of (12a,b) in (10) and (9) completes the evaluation of rolling moment, for dissimilar vortices and zero bank angle. The opposite case of similar vortices and non-zero bank angle has been considered elsewhere [21]. The bank angle correction became important if the aircraft roll significantly as a consequence of the wake encounter.

3 Roll equation with damping and controls

For substitution in the roll dynamics equation, including the effects of aerodynamic damping and flight controls, the rolling moment induced by the pair of dissimilar HB-vortices is used in the form (9), where the dimensionless encounter factors h_r, h_l, (10) are specified by (12a,b), viz.:

$$h_r = 2 + (y_r/b) h_{1r} - 2(a_r/b) h_{2r} + (\lambda - 1)\left\{1 + 2\left[\left(y_r^2 - a_r^2\right)/b^2\right] h_{4r} - 8\left(a_r y_r / b^2\right) h_{3r}\right\}, \quad (13)$$

where:

$$h_{1r} = \log\left\{\left[(b/2 - y_r)^2 + a_r^2\right] / \left[(b/2 + y_r)^2 + a_r^2\right]\right\}, \quad (14a)$$

$$h_{2r} = \arctan\left[(b/2 + y_r)/a_r\right] + \arctan\left[(b/2 - y_r)/a_r\right], \quad (14b)$$

$$h_{3r} = 2\arctan(y_r/a_r) + \arctan\left((b/2 - y_r)/a_r\right) - \arctan\left((b/2 + y_r)/a_r\right) \quad (14c)$$

$$h_{4r} = \log\left\{\left[\left(a_r^2 + b^2/4 + y_r^2\right)^2 - b^2 y_r^2\right] / \left(a_r^2 + y_r^2\right)^2\right\}. \quad (14d)$$

Note that the last three terms on the r.h.s. of (13) vanish for a rectangular wing $\lambda = 1$. The average dimensionless encounter factor h is defined by:

$$\Omega_r a_r^2 h_r - \Omega_l a_l^2 h_l \equiv (\Omega_r - \Omega_l) a^2 h, \quad (15)$$

where a is taken to be the mean vortex radius:

$$a \equiv (a_r + a_l)/2. \quad (16)$$

The simplest case is that of vortices with equal radii $a_r = a_l = a$, symmetrically placed $y_r = -y_l = y_0$ when $h_r = h_l = h$; in general $h_r \neq h_l$, for a asymmetrically placed vortices $y_r \neq -y_l$ with distinct vortex radii $a_r \neq a_l$, and the average encounter factor is defined by (15).

Substitution of (15) specifies (9) the rolling moment:

$$R = -\frac{C_{L_\alpha} \rho U S_2}{1+\lambda} a^2 h \Omega(t), \quad (17)$$

whose time dependence is specified by that of the sum of the vorticities of the right and left vortices:

$$2\Omega(t) \equiv \Omega_r(t) - \Omega_l(t). \quad (18)$$

These time dependences are similar [7] for identical vortex radii:

$$a_l = a_r \equiv a: \ \Omega(t) = \frac{\Gamma_0}{2\pi\eta t}\exp\left(-\frac{a^2}{2\eta t}\right), \quad (19)$$

where the wake vortex circulation strength [22] is specified by:

$$\Gamma_0 = \frac{c_{r_1} W_1}{\rho U_1 S_1}, \quad (20)$$

and the index "1" applies to the leading aircraft.

Substitution of (20) into (19) specifies the time dependence (17) of the induced rolling moment:

$$R = -\frac{2h}{1+\lambda}\frac{C_{L_\alpha}}{2\pi} W_1 \frac{U_2}{U_1}\frac{S_2}{S_1} c_{r_1} \frac{a^2}{\eta t}\exp\left(-\frac{a^2}{2\eta t}\right), \quad (21)$$

which appears in the roll dynamics equation, with one degree-of-freedom, i.e. no coupling to other axis:

$$I_2\ddot{\phi} - \frac{1}{2}\rho U_2 S_2 (b_2)^2 C_{\dot{\phi}}\dot{\phi} = \rho S_2 b_2 (U_2)^2 C_\delta \delta(t) - \frac{2h}{1+\lambda}\frac{C_{L_\alpha}}{2\pi} W_1 \frac{U_2}{U_1}\frac{S_2}{S_1} c_{r_1}\frac{a^2}{\eta t}\exp\left(-\frac{a^2}{2\eta t}\right). \quad (22)$$

Writing the roll moment of inertia in terms of mass and radius of gyration:

$$I_2 = m(r_2)^2 = W_2 (r_2)^2 / g, \quad (23)$$

leads to the roll dynamics equation in the form:

$$\ddot{\phi} - \frac{1}{2}\frac{\rho U_2 S_2}{W_2/g}\left(\frac{b_2}{r_2}\right)^2 C_{\dot{\phi}}\dot{\phi} = \frac{\rho S_2 b_2}{W_2/g}\left(\frac{U_2}{r_2}\right)^2 C_\delta \delta(t) - \frac{2h}{1+\lambda}\frac{C_{L_\alpha}}{2\pi}\frac{W_1}{W_2}\frac{S_2}{S_1}\frac{U_2}{U_1}\left(\frac{a}{r_2}\right)^2 \frac{c_{r_1} g}{\eta t}\exp\left(-\frac{a^2}{2\eta t}\right). \quad (24)$$

4 Aileron schedule to compensate vortex encounter

The simplest result to follow from (24) is that there will be no roll motion, i.e. the wake vortex encounter will be compensated by the aileron deflection as a function of time specified by:

$$\delta(t) = \frac{1}{C_\delta}\frac{2h}{1+\lambda}\frac{C_{L_\alpha}}{2\pi}\frac{W_1}{\rho b_2 S_1}\frac{c_{r_1} g}{U_1 U_2}\exp\left(-\frac{a^2}{2\eta t}\right). \quad (25)$$

Thus the aileron deflection needed to compensate the wake vortex encounter is given by (25) as a product of dimensionless factors, showing that it increases: (i) for smaller aileron rolling moment coefficient C_δ; (ii) for larger mean encounter parameter h defined in (15); (iii) for smaller taper ratio of following aircraft λ in (3a), noting it also appears in (13); (iv) for larger leading aircraft wing loading W_1/S_1 (hence stronger wake), smaller air density ρ (e.g. higher altitudes) and smaller following aircraft span b_2 (i.e. smaller roll moment arm); (v) for larger vortex core radius a squared, divided by viscosity η multiplied by time t, so that larger viscosity and longer time, which cause wake decay, also reduce required compensation by aileron deflection; (vi) for larger root chord of leading aircraft (hence stronger wake) multiplied by the acceleration of gravity g, to be dimensionless when divided by the product of the velocities of the leading and following aircraft. So the aileron deflection required to compensate wake effects increases for slower leading aircraft (hence stronger wake) and slower following aircraft (lower roll control effectiveness).

The last exponential factor in (25), is the same as in the vorticity (19,20), and shows that its peak occurs at the time:

$$t_* = a^2/2\eta, \; \Omega_{max} = \Omega(t_*) = \frac{\Gamma_0}{\pi a^2 e} = \frac{c_{r_1} W_1}{e\pi\rho U_1 S_1 a^2}, \quad (26a,b)$$

and the corresponding aileron deflection would occur at the same time:

$$\delta_* \equiv \delta(t_*) = \frac{2}{e}\frac{h}{1+\lambda}\frac{C_{L_\alpha}}{2\pi}\frac{1}{C_\delta}\frac{W_1}{\rho b_2 S_1}\frac{c_{r_1} g}{U_1 U_2}. \quad (27)$$

The aileron deflection for wake vortex compensation at peak vorticity increases with: (i) larger encounter factor h in (15); (ii) smaller wing taper ratio λ of following aircraft; (iii) smaller aileron rolling moment coefficient; (iv) larger wing loading W_1/S_1, of leading aircraft; (v) smaller air density, due to smaller aerodynamic forces; (vi) smaller following aircraft span, due to smaller moment arm; (vii) larger root chord c_{r_1} of leading aircraft, due to stronger wake; (viii) smaller speed of leading aircraft U_1 due to stronger wake; (ix) smaller speed of the following aircraft, due to reduced roll control effectiveness.

As an example, the case of two Boeing 757-200 flying one behind the other is considered. The data needed to calculate the maximum aileron deflection is given in *Table I*, with basic data from open sources [23,24] at the top, and at the bottom, data derived by calculation using the formulas in this paper. The vortex core radius was taken to be 3% of the wing span. The peak aileron deflection is specified by (27), viz. $\delta_* = 4.50^\circ$. The ratio:

$$\delta_{max}/\delta_* = \Omega/\Omega_{max} = 4.4, \quad (28)$$

specifies the fraction of the peak vorticity the following aircraft can cope with; the smaller the fraction of the peak vorticity the following aircraft can cope with, the larger must be the separation distance, for the vorticity to have decayed by that much.

5 Free response and aileron deflection

The preceding case (§4) of an aileron control law which compensates the wake vortex encounter is the only situation in which there is no aircraft roll response, because the forced response to the ailerons (ii) exactly balances the response to the wake vortex (iii), leaving only the free response (i), which is zero if there are no initial perturbation. The three terms of the response (i,ii,iii) are calculated next in turn, starting with the free response $\phi_1(t)$, which is the solution of the roll equation (24) without forcing terms on the r.h.s., viz.:

$$\ddot{\phi}_1 + \overline{\mu}\dot{\phi}_1 = 0\,, \tag{29}$$

where the overall damping coefficient is specified by:

$$\overline{\mu} \equiv -\frac{1}{2}\frac{\rho U_2 S_2}{W_2/g}\left(\frac{b_2}{r_2}\right)^2 C_{\dot{\phi}}\,, \tag{30}$$

and the damping time by $1/\overline{\mu}$. The damping increases with: (i) the ratio of span to gyration radius squared; (ii) the roll damping coefficient $C_{\dot{\phi}}$; (iii) the air density (lower altitude), airspeed and wing area divided by the mass. The roll damping coefficient $C_{\dot{\phi}}$, the overall damping coefficient $\overline{\mu}$ in (30) in seconds^{-1}, and the damping time $1/\overline{\mu}$ are indicated in the third panel of *Table I*.

The solution of (29) is the free response:

$$\phi_1(t) = A + Be^{-\overline{\mu}t}\,, \tag{31}$$

where the constants of integration A, B are determined from the initial bank angle ϕ_0 and roll rate $\dot{\phi}_0$ at time zero:

$$\phi_0 \equiv \phi_1(0) = A + B, \quad \dot{\phi}_0 = \dot{\phi}_1(0) = -\overline{\mu}B\,. \tag{32}$$

It follows that the free response (31) is given by:

$$\phi_1(t) = \phi_0 + (\dot{\phi}_0/\overline{\mu})\left[1 - e^{-\overline{\mu}t}\right], \tag{33}$$

for arbitrary initial bank angle ϕ_0 and roll rate $\dot{\phi}_0$.

The forced response to the ailerons $\phi_2(t)$ is even simpler, since it is a particular solution of the roll dynamics equation (24), omitting the last term on the r.h.s. side representing wake vortex effects:

$$\ddot{\phi}_2 + \overline{\mu}\dot{\phi}_2 = \nu\,, \tag{34}$$

where the aileron deflection was taken to be maximum:

$$\nu \equiv \frac{\rho S_2 b_2}{W_2/g}\left(\frac{U_2}{r_2}\right)^2 C_\delta \delta_{\max}\,. \tag{35}$$

The forcing term increases with: (i) the air density times span and wing area (which is the mass of a parallelepiped of air, with base area equal to the wing area and height equal to the span) divided by the aircraft mass, specifying a relative density [7]; (ii) the square of airspeed divided by the radius of gyration; (iii) the aileron rolling moment coefficient; (iv) the aileron deflection taken at maximum value for fastest response. The forced response to constant aileron deflection is a bank angle varying linearly with time:

$$\phi_2(t) = \frac{\nu}{\overline{\mu}}t \equiv -2\frac{U_2}{b_2}\frac{C_\delta}{C_{\dot{\phi}}}\delta_{\max}t\,, \tag{36}$$

showing that in the presence of damping the roll rate is constant $\dot{\phi}_2(t) = -\nu/\overline{\mu}$, and increases with: (i) the airspeed divided by the span; (ii) the ratio of the aileron rolling moment coefficient C_δ to the dimensionless aerodynamic roll damping coefficient $C_{\dot{\phi}}$; (iii) the maximum aileron deflection. The forcing factor ν in (34) and the rolling moment coefficient C_δ and the roll rate due to maximum aileron deflection $\dot{\phi}_2$ are indicated in the fourth panel of *Table I*. Note that in the absence of damping:

$$\mu = 0: \qquad \ddot{\phi}_2 = \nu\,, \tag{37}$$

the roll acceleration would be constant, and hence the roll rate would be linear function of time (38a):

$$\dot{\phi}_2(t) = \nu t, \qquad \phi_2(t) = \frac{1}{2}\nu t^2\,, \tag{38a,b}$$

and the bank angle a quadratic function of time (38b).

6 Response forced by wake encounter

The response to the wake encounter would be almost as simple as for constant aileron deflection (§5) if the induced rolling moment is taken to be constant [25]. Taking into account the dependence of the induced rolling moment on time leads to a less simple response $\phi_3(t)$, specified by a particular integral of the roll dynamics equation (24), without the first term on the r.h.s.:

$$\ddot{\phi}_3 + \bar{\mu}\dot{\phi}_3 = -\bar{\xi} t^{-1} \exp\left(-a^2/2\eta t\right), \tag{39}$$

where the vortex wake effect is specified by:

$$\bar{\xi} \equiv \frac{2h}{1+\lambda} \frac{C_{L_\alpha}}{2\pi} \frac{W_1/S_1}{W_2/S_2} \frac{U_2}{U_1} \left(\frac{a}{r_2}\right)^2 \frac{c_{r_1} g}{\eta}, \tag{40}$$

and increases for : (i) larger encounter factor h and smaller taper ratio λ; (ii) larger ratio of wing loading of the leading aircraft to the wing loading of the following aircraft: (iii) larger ratio airspeed of following aircraft (catches wake sooner) to the airspeed of the leading aircraft (leaves stronger wake for lower airspeed); (iv) larger square ratio of vortex core radius to radius of gyration, i.e. larger vortex and mass further inboard; (v) larger root chord of leading aircraft, leading to larger wake vortex strength (20); (vi) smaller viscosity leading to slower vortex decay.

It is convenient to introduce a dimensionless time divided by the time (26a) of peak vorticity:

$$\tau \equiv t/t_* = 2\eta t/a^2, \quad \Phi(\tau) = \phi_3(t), \tag{41a,b}$$

so that the roll response forced by the wake vortex satisfies:

$$\ddot{\Phi} + \mu\dot{\Phi} = -(\xi/\tau) e^{-1/\tau}, \tag{42}$$

where the dimensionless aerodynamic damping (30) and vortex effect (40) are given respectively by:

$$\mu \equiv \frac{\bar{\mu} a^2}{2\eta} = -\frac{1}{4}\left(\frac{b_2}{r_2}\right)^2 \frac{\rho S_2 a}{W_2/g} \frac{U_2 a}{\eta} C_{\dot{\phi}}, \tag{43a}$$

$$\xi \equiv \frac{\bar{\xi} a^2}{2\eta} = \frac{2h}{1+\lambda} \frac{C_{L_\alpha}}{2\pi} \frac{W_1/S_1}{W_2/S_2} \frac{U_2}{U_1} \left(\frac{a}{r_2}\right)^2 \frac{c_{r_1} a^2 g}{2\eta^2}. \tag{43b}$$

The forced solution of (42) is sought by the method of variation of parameters, i.e. as the free solution (31) with non-constant coefficients:

$$\Phi(\tau) = A(\tau) + B(\tau) e^{-\mu\tau}, \tag{44}$$

which can be chosen at will.

Substitution of (44) into (42) yields:

$$-(\xi/\tau) e^{-1/\tau} = \left(\ddot{A} + \mu\dot{A}\right) + \left(\ddot{B} - \mu\dot{B}\right) e^{-\mu\tau}, \tag{45}$$

which is satisfied in particular by:

$$A(\tau) = 0, \quad \dot{B} - \mu B = -\xi \int \tau^{-1} e^{-1/\tau} e^{\mu\tau} d\tau, \tag{46a,b}$$

viz. the first arbitrary function is not needed (46a), and the second satisfies a first-order differential equation (46b), for which a particular solution is obtained again by the method of variation of parameters:

$$B(\tau) = D(\tau) e^{\mu\tau}; \tag{47a}$$

substitution of (47a) in (46b) specifies the function $D(\tau)$ by:

$$-\xi \int \tau^{-1} e^{-1/\tau} e^{\mu\tau} d\tau = \dot{B} - \mu B = \dot{D} e^{\mu\tau}. \tag{47b}$$

Integration of (47b) and substitution in (47a), leads together with (46a) to (44) the forced response:

$$\Phi(\tau) = D(\tau) = -\xi \int e^{-\mu\tau} d\tau \int \tau^{-1} e^{-1/\tau} e^{\mu\tau} d\tau, \tag{48}$$

to the wake vortex.

7 Time evolution of the forced response

The total roll response is the sum of the free response (33) with the forced responses to the ailerons (36) and the wake vortex (41b):

$$\phi(t) = \phi_1(t) + \phi_2(t) + \phi_3(t). \tag{49}$$

Assuming that the initial bank angle and the roll rate are zero there is no free response $\phi_1(t) = 0$ in (33), and the total forced response

$$\phi_0 = 0 = \dot{\phi}_0: \quad \phi(t) = \phi_2(t) + \Phi\left(2\eta t/a^2\right), \tag{50}$$

consists of: (i) the response to the ailerons, given explicitly by (36) in the presence of damping , and by (38b) in the absence of damping; (ii) the response to the wake vortex, which in the presence of damping is given by (48), and in the absence of damping is expressed in terms of the exponential integral [15]:

$$T = 1/\tau: \; E_0(T) \equiv \int_T^\infty T^{-1} e^{-T} dT = \int_0^{1/\tau} \tau^{-1} e^{-1/\tau} d\tau = E_0(1/\tau), \tag{51}$$

by (48) with $\mu = 0$:

$$\mu = 0: \quad \Phi_0(\tau) = -\xi \int d\tau \int d\tau \; e^{-1/\tau} \tau^{-1} = -\xi \int E_0(1/\tau)\, d\tau, \tag{52}$$

in agreement with [8].

Since the dimensionless roll rate in the absence of damping (52) is specified by an exponential integral of order zero:

$$-\xi^{-1}\dot{\Phi}_0(\tau) = E_0(1/\tau) = \int \tau^{-1} e^{-1/\tau} d\tau \,, \qquad (53)$$

the comparison with the dimensionless roll rate in the presence of damping (48)

$$-\xi^{-1}\dot{\Phi}(\tau) = e^{-\mu\tau} \int \tau^{-1} e^{-1/\tau} e^{\mu\tau} d\tau \,, \qquad (54)$$

suggests considering the integral:

$$\begin{aligned} H &\equiv -\left[e^{\mu\tau}\dot{\Phi}(\tau) - \dot{\Phi}_0(\tau)\right] \\ &= \int \tau^{-1} e^{-1/\tau}\left(e^{\mu\tau}-1\right) d\tau/\xi \end{aligned} . \qquad (55)$$

Expanding the exponential in power series leads to:

$$H = \sum_{n=1}^{\infty} \frac{\mu^n}{n!} \int e^{-1/\tau} \tau^{n-1} d\tau \,, \qquad (56)$$

where the coefficients are exponential integrals of order n:

$T = 1/\tau$:

$$\int_0^{1/\tau} e^{-1/\tau} \tau^{n-1} d\tau = \int_T^{\infty} T^{-1-n} e^{-T} dT \equiv E_n(1/\tau) \,, \qquad (57)$$

and thus:

$$H = \sum_{n=1}^{\infty} \frac{\mu^n}{n!} E_n(1/\tau) . \qquad (58)$$

Substituting (58) and (53) in (55) yields:

$$\dot{\Phi}(\tau) = -\xi e^{-\mu\tau}\left\{E_0(1/\tau) + \sum_{n=1}^{\infty} \frac{\mu^n}{n!} E_n(1/\tau)\right\} , \qquad (59)$$

which specifies the dimensionless roll response:

$$\Phi(\tau) = -\xi \sum_{n=0}^{\infty} \frac{\mu^n}{n!} \int e^{-\mu\tau} E_n(1/\tau)\, d\tau \,, \qquad (60)$$

as a series of powers of the damping, with exponential integrals of order n as coefficients. If the damping is weak, only the first terms of the series are needed, e.g. the first two for $\mu^2 << 1$.

8 Identical and aligned leading and following aircraft

The forced response to the wake vortex, is represented by roll rate and bank angle plotted in *Figures 2* and 3, for identical leading and following aircraft of Boeing 757-200 type. The Figure 2 plots (top) the dimensionless roll rate (59) and (bottom) the bank angle (60) versus dimensionless time $0 \le \tau \le 20$ corresponding (41a) to $0 \le t \le 20 t_*$ twenty times peak vorticity time. It is seen that the roll rate (Figure 2, top) increases initially due to the wake vortex encounter, and decays ultimately due to roll damping; the peak roll rate occurs at $\tau = 2.22$, i.e. at about twice the peak vorticity time. Since Figure 2 plots (59,60), i.e. the roll response (41a,b) with damping, but without aileron reflection, it is clear from (39), that, for long time $t \to +\infty$ or $t >> \tau$, the r.h.s. vanishes, leading to: (i) a zero roll rate $\dot{\Phi} \to 0$ as $\tau \to +\infty$ in Figure 2, top; (ii) a constant asymptotic bank angle $\Phi(\tau) = \phi_3(t) \to \phi_3(t) \equiv \phi_\infty$ as $\tau \to +\infty$ in Figure 2, bottom. The asymptotic bank angle is a measure of the effect on the following aircraft of the wake of the leading aircraft. The Figure 2 bottom shows that the bank angle increases monotonically with time during the vortex encounter to a constant asymptotic value $\Phi \to \phi_\infty$ as the dimensionless time becomes large $\tau > 10$. These results are confirmed in Figure 3, by the roll rate (top) peaking at $t = 4.3\,s$ after the vortex encounter, and decaying to a small value after $t > 20\,s$, to an asymptotic bank angle (bottom) of $\phi_\infty = 12.5^\circ$.

The Figure 4 shows the contrast between the undamped roll response, which diverges rapidly, and the damped roll response which tends to a constant bank angle. The value $\phi_\infty = 12.5^\circ$ is just above the threshold $\phi_{\max} = 10^\circ$ for which airline procedures regarding passenger comfort require a go-round on approach to land. Since the asymptotic bank angle does not include the effect of aileron deflection, it is clear that roll control could be used to keep the bank angle below the threshold. The Figure 5 shows the sum of the first $N+1$ terms of the series (60), viz.:

$$\phi_3^N(t) \equiv \Phi^N(\tau) = -\xi \sum_{n=0}^{N} \frac{\mu^n}{n!} \int e^{-\mu\tau} E_n(1/\tau)\, d\tau\,, \quad (61)$$

for several values of N. The first two terms $N=1$ of the series solution (60) to $O(\mu)$ give an error of less than 20% in the bank angle response, and the first three terms $N=2$ or $O(\mu^2)$ give an error of less than 2%. This can be confirmed from Table II, which indicates the asymptotic bank angle $\phi_\infty^N \equiv \phi_3^{(N)}(\infty)$ calculated with $N+1$ terms (61) of the series (60), and shows rapid convergence for $N \geq 2$. The Figure 6 shows the bank angle response for the same aircraft, replacing the actual roll damping $\mu = 0.5$, by larger and smaller hypothetical values, up to the double and a half, and half-way between. It is clear that stronger damping leads to a smaller asymptotic bank angle, which is established sooner, as indicated in Table III.

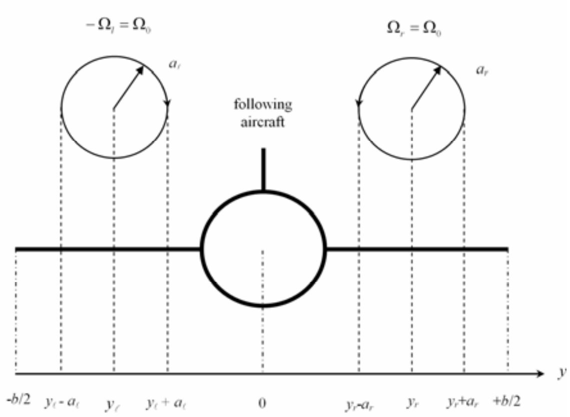

Figure 1- Interaction of following aircraft with two wing tip vortices of leading aircraft, with parallel axis and asymmetric positions and different radii and vorticities.

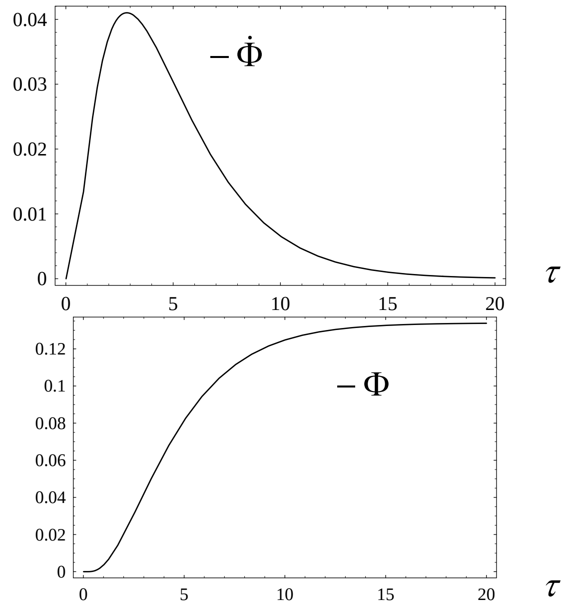

Figure 2- Roll rate (top) and bank angle (bottom), as function of time made dimensionless by dividing by peak vorticity time, for wake vortex encounter between identical leading and following aircraft of type (Boeing 757-200).

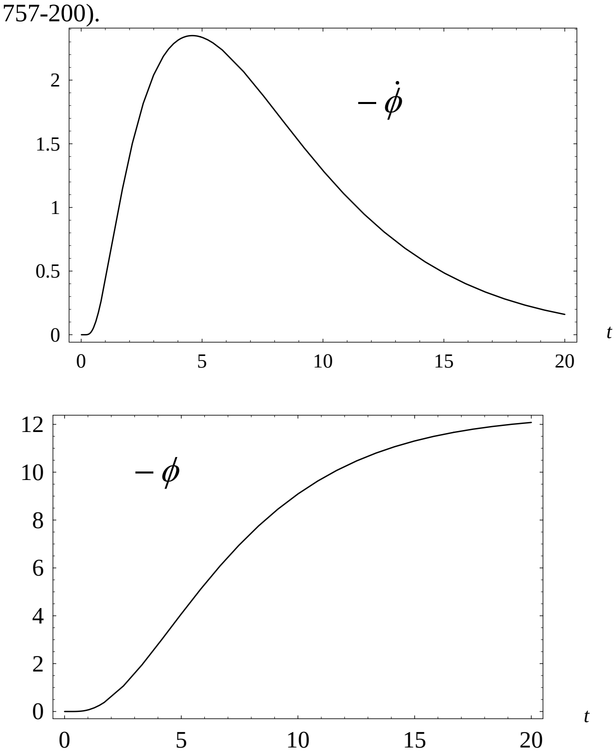

Figure 3- Roll rate (top) and bank angle (bottom) as a function of time for wake vortex encounter between leading and following aircraft both of the same type (B757-200).

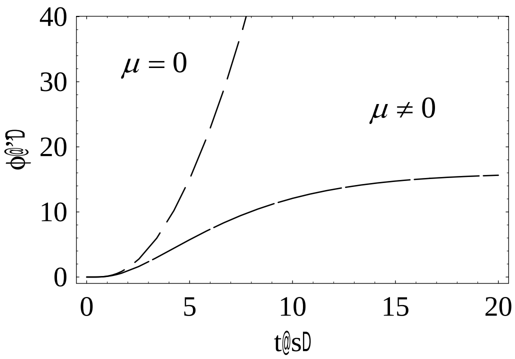

Figure 4- Bank angle as a function of time for Boeing 757-200 encountering the wake of a similar aircraft, without (dotted line) and with (solid line) damping.

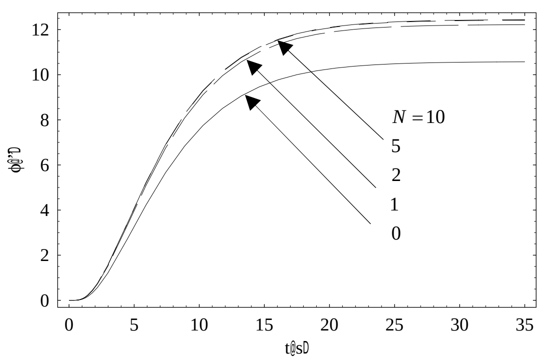

Figure 5- Bank angle response due to wake vortex encounter of identical leading and following Boeing 757-200 aircraft, calculated from the exact series solution (60), truncated with $N = 0,1,2,5,10$ terms.

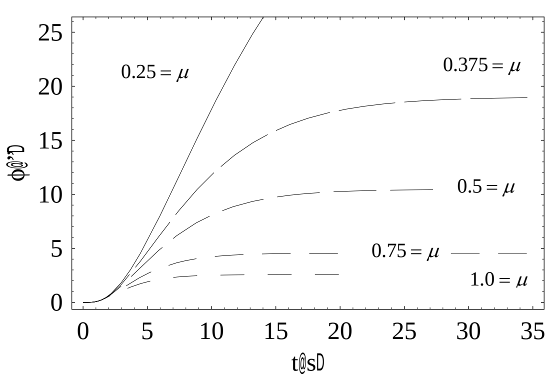

Figure 6- Exact bank angle response of identical leading and following Boeing 757-200 aircraft, replacing the roll damping coefficient $\mu = 0.5$ by hypothetical larger and smaller values.

Acknowledgement

This work has been supported by the project S-Wake of CEC Aeronautics programme and has benefited from comments of other partners in this activity. The second author acknowledges the Ph.D. grant SFRH/BD/3104/2000 from "Fundação para a Ciência e a Tecnologia".

References

[1] Shen, S, Ding, F, Han, J., Lin, Y-L., Arya, S. P. & Proctor, F. H. 1999 "Numerical modeling studies of wake vortices: real case simulations", AIAA Paper 99-0755, 37th Aerospace Sciences Meeting, Reno, Nevada.

[2] Vicroy, D. D. & Nguyen, T. 1993 "A numerical simulation study to develop an acceptable wake encounter boundary for a B737-100 airplane", AIAA paper.

[3] Perry, R. R., Hinton, D. A. & Stuever, R. A. 1996 "NASA wake vortex research for aircraft spacing" AIAA paper.

[4] Hinton, D.A. 1996 "An Aircraft Vortex Spacing System

[5] Hinton, D.A., Charnock, J.K., Bagwell, D.R. & Grigsby, D. 1999 "NASA Aircraft Vortex Spacing System Development Status", AIAA 37th Aerospace Sciences Meeting, Reno, Nevada.

[6] Jackson, W. (ed) 2001 "Wake Vortex Prediction: An Overview, Appendix F: Hazard Definition", Transportation Department of Canada TP 13629E.

[7] Campos, L.M.B.C. & J.M.G. Marques 2004 "On the calculation of safe separation distances between aircraft due to turbulent wakes" (in preparation).

[8] Campos, L.M.B.C. & J.M.G. Marques 2004 "On wake vortex response for all combinations of five classes of aircraft", Paper 2718, pages 295-310.

[9] McGowan, W. A., "Calculated Normal Load Factors on Light Airplanes Traversing the Trailing Vortices of Heavy Transport Airplanes", NASA TN D-829, May 1961.

[10] Iversen, J. D., and Bernstein, S., "Trailing Vortex Effects on Following Aircraft", AIAA

Journal of Aircraft, Vol. 11, No. 1, Jan. 1974, pp. 60-61.
[11] Nelson, R. C., "The Dynamic Response of Aircraft Encountering Aircraft Wake Turbulence", Tech. Report AFFDL-TR-74-29, Air Force Flight Dynamics Laboratory, Wright-Patterson Air Force Base, Ohio, June 1974.
[12] Sammonds, R. I., and Stinnett, G. W., Jr., "Hazard Criteria for Wake Vortex Encounters", NASA TM X-62,473, Aug. 1975.
[13] Sammonds, R. I., Stinnett, G. W., Jr., and Larsen, W. E., "Wake Vortex Encounter Hazard Criteria for Two Aircraft Classes", NASA TM X-73,113, June 1976. (Also FAA-RD-75-206.)
[14] Nelson, R. C., "Dynamic Behavior of an Aircraft Encountering Wake Turbulence", AIAA Journal of Aircraft, Vol. 13, No. 9, Sept. 1976, pp. 704-708.
[15] McWilliams, I. G., "Hazard Extent About Aircraft Trailing Wake Vortices-Analytic Approach", Proceedings of the Aircraft Wake Vortices, Conference, edited by J. N. Hallock, Report No. FAA-RD-77-68, U. S. Dept. of Transportation, March 15-17, 1977, pp. 23-30.
[16] Tinling, B. E., "Estimation of Vortex-Induced Roll Excursions Based on Flight and Simulation Results", Proceedings of the Aircraft Wake Vortices Conference, edited by J. N. Hallock, Report No. FAA-RD-77-68, U. S. Dept. of Transportation, March 15-17, 1977, pp 11-22.
[17] Tinling, B. E., "Estimates of the Effectiveness of Automatic Control in Alleviating Wake Vortex Induced Roll Excursions", NASA TM-73,267, Aug. 1977.
[18] McMillan, O. J., Nielsen, J. N., Schwind, R. G., and Dillenius, M. F. E., "Rolling Moments in a Trailing-Vortex Flow Field", AIAA Journal of Aircraft, Vol. 15, No. 5, May 1978, pp. 280-6.
[19] Rossow, V. J., and Tinling, B. E., "Research on Aircraft/Vortex-Wake Interactions to Determine Acceptable Level of Wake Intensity", AIAA Journal of Aircraft, Vol. 25, No. 4, June 1988, pp. 481-492.
[20] Hallock, J.N. & Burnham, D.C. 1997 Decay characteristics of wake vortex from jet transport aircraft AIAA paper 97-0060, 35th Aerosp. Sci. Meet. Exhib. 9-10 Jan., Reno, NV.
[21] Tatnall, C.R. 1995 "A proposed methodology for determining wake-vortex imposed aircraft separation constraints", M. Sc. thesis submitted at George Washington University.

[22] Hinton, D.A. & Tatnall, C.R. 1997 "A Candidate vortex strength definition for application to the NASA Aircraft Vortex Space System (AVOSS)" NASA Tech. Memo TM-110343.

[23] Jackson, P. 2000 *Jane´s All-the-World's Aircraft* 2000-2001. MacDonald and Jane's, London.

[24] Stuever, R.A. Airplane data base for wake-vortex hazard definition and assessment, version 2.0, NASA Langley Research Center.
[25] Belotserkovsky, A. 2001 "Hazard Definition", Appendix F, in "Wake Vortex Prediction: An Overview", W. Jackson (ed), Dept. Transp. Canada TP13629.
[26] Abramowitz, M., Stegun, I. 1965 *Tables of mathematical functions*. Dever.